



Potential mechanisms underlying the effect of hepatocyte growth factor on liver injury in short bowel syndrome model rats

Koshiro Sugita¹ · Keisuke Yano¹ · Makoto Matsukubo² · Yumiko Iwamoto¹ · Masato Ogata¹ · Lynne Takada¹ · Chihiro Kedoin¹ · Masakazu Murakami¹ · Toshio Harumatsu¹ · Shun Onishi¹ · Takafumi Kawano¹ · Mitsuru Muto¹ · Kotaro Kumagai³ · Akio Ido³ · Tatsuru Kaji⁴ · Satoshi Ieiri¹

Accepted: 3 November 2023

© The Author(s), under exclusive licence to Springer-Verlag GmbH Germany, part of Springer Nature 2023

Abstract

Purpose The purpose of this study was to investigate the autophagy associated with apoptosis in hepatic damage in the short bowel syndrome rat model.

Methods SD rats underwent jugular vein catheterization for continuous total parenteral nutrition (TPN) and 90% small bowel resection. Animals were divided into two groups: TPN plus SBS (Control group) or TPN plus SBS plus intravenous administration of HGF (HGF group). On day 7, the rats were harvested, and hepatocellular injury was evaluated.

Results In an SBS rat model, hepatic steatosis and lobular inflammation were histologically suppressed in the HGF group ($p < 0.01$). The expression of tumor necrosis factor- α in the HGF group tend to be higher than that in the control group ($p = 0.13$). The gene expression of transforming Growth Factor- β in the HGF group was suppressed compared to the control group ($p < 0.01$). HGF treatment may have an antiapoptotic effect via the intrinsic pathway by caspase 9. Protein expressions of Rubicon ($p = 0.03$) and p62 ($p < 0.01$) in the HGF group were found to have increased compared to those in the control group.

Conclusion The inhibitory effect of HGF on hepatic steatosis remains unclear, and further studies focusing on the mechanisms of fat accumulation are needed.

Keywords Hepatic steatosis · Short bowel syndrome · Hepatocyte growth factor · Apoptosis · Autophagy

Abbreviations

IFALD	Intestinal failure-associated liver disease
SBS	Short bowel syndrome
NAFLD	Nonalcoholic fatty liver diseases
HGF	Hepatocyte growth factor
TPN	Total parenteral nutrition
IL6	Interleukin-6
TNF α	Tumor necrosis factor- α
TGF β	Transforming growth factor- β
BAX	Bcl-2-associated X protein

Koshiro Sugita and Keisuke Yano contributed equally to this work.

✉ Satoshi Ieiri
sieiri@m.kufm.kagoshima-u.ac.jp

Koshiro Sugita
ksugita@m.kufm.kagoshima-u.ac.jp

¹ Department of Pediatric Surgery, Research Field in Medical and Health Sciences, Medical and Dental Area, Research and Education Assembly, Kagoshima University, 8-35-1, Sakuragaoka, Kagoshima City 890-8520, Japan

² Department of Pediatric Surgery, Kagoshima City Hospital, Kagoshima, Japan

³ Digestive and Lifestyle Diseases, Department of Human and Environmental Sciences, School of Medical and Dental Sciences, Kagoshima University Graduate, Kagoshima, Japan

⁴ Department of Pediatric Surgery, Kurume University School of Medicine, Kurume, Japan

Introduction

Intestinal failure-associated liver disease (IFALD) is a life-threatening complication in patients with short bowel syndrome (SBS), who require long-term parenteral nutrition. The pathogenesis of IFALD is complex according to the multi-hit theory, and elucidating its pathogenesis and drug development remain as major challenges for pediatric

surgeons. The hepatic steatosis that occurs in IFALD is histologically similar to nonalcoholic fatty liver diseases (NAFLD) in adults. However, IFALD in children occurs against the background of intestinal failure. Therefore, unlike NAFLD and nonalcoholic steatohepatitis in adults, inflammation and biliary stasis with hepatic steatosis in the early stages of IFALD development and sometimes rapid progression are issues that need to be resolved.

Our research group has focused on HGF, which has been reported to have anti-inflammatory effects which can thus inhibit hepatic steatosis [1–3]. Our previous studies suggested that HGF suppresses hepatic steatosis via the intrinsic pathway in a parenterally fed rat model [4] and via the gut microbiota and farnesoid X receptor in a rat model of SBS [5]. However, the underlying mechanisms of hepatic steatosis remain unclear. In this study, we investigated the autophagy associated with apoptosis in hepatic damage in the short bowel syndrome rat model.

Materials and methods

Animals

Our experimental rats were 7-week-old male Sprague–Dawley (SD) rats weighing 200–240 g (Kyudo Co., Ltd., Saga, Japan). The rats were acclimatized to the animal laboratory environment for seven days before undergoing the experiments. During this period, the rats were individually housed in metabolic cages with ad libitum access to standard rat chow and water. The environment for the rats was maintained at a standardized temperature (23 ± 1 °C) and humidity ($50\% \pm 10\%$) with a 12-h light–dark cycle (lights on at 7:00 a.m.).

Study design

The animals were randomly divided into 2 groups as follows: massive small bowel resection and total parenteral nutrition (TPN) (SBS/TPN: control group, $n=9$); SBS/TPN with the intravenous administration of rh-HGF (Eisai Co., Ltd., Tokyo, Japan) (SBS/TPN/HGF: HGF group, $n=9$). The dose of rh-HGF was set at 0.3 mg/kg/day based on the findings of our previous study [4, 6, 7]. Rh-HGF was dissolved in saline and administered daily as a single intravenous infusion via a central venous catheter. On day 7, blood and liver tissue specimens were harvested for biochemical and histological analyses.

Surgical procedures and maintenance methods

Under anesthesia with isoflurane (1.5% inhalation by mask), all rats underwent catheterization using the cut-down method

through the right jugular vein, and then the catheter was tunneled out of the back and attached to a standard swivel device using the same methods. After catheterization, all rats underwent 90% small bowel resection, leaving 5 cm of the ileum above the ileocecal valve anastomosed to the jejunum and 5 cm below the ligament of Treitz. The rats received cefazolin (50 mg/kg per dose, subcutaneously; Otsuka Pharmaceutical Factory, Inc., Tokushima, Japan) to prevent any postoperative infection, and buprenorphine (0.01 mg/kg per dose, subcutaneously; Otsuka Pharmaceutical Factory, Inc.) for analgesia. The rats were allowed ad libitum access to water immediately after surgery. TPN was delivered using a multichannel syringe pump (KDS Legato 200 Series Syringe Pump Series; KD Scientific, Inc., Holliston, MA, USA). After catheterization, the rats were maintained with a low-concentration NEOPAREN® No. 2 (Otsuka Pharmaceutical Co., Ltd.) TPN solution (60 mL/day), to which 20% Intralipos® (Otsuka Pharmaceutical Co., Ltd.) was added. The composition of the TPN solution was as follows (g/L): amino acids 25, dextrose 145, and soybean oil 33.3. The solution also contained the following electrolytes (final mmol/L): 41.6 Na^+ , 22.5 K^+ , 41.6 Cl^- , 4.1 Ca^{2+} and 4.1 Mg^{2+} . After 24 h, the composition of the TPN solution was changed to the following (in g/L): amino acids 31.6, glucose 203, and soybean oil 33.3, with similar electrolyte additives. The TPN solution was delivered at a rate of 60 mL/d. This provided equivalent isocaloric/isonitrogenous nutritional support to all TPN-fed rats, consisting of 76.4 kcal/rat/day (1.9 g protein, 2.0 g fat, and 12.2 g carbohydrate). On day 7, all rats were anesthetized by isoflurane inhalation and then were euthanized by exsanguination and blood collection. Liver tissue was harvested, rinsed in cold saline, and fixed in a 10% formaldehyde-neutral buffer solution for 24 h.

Biochemical tests

The collected blood was immediately centrifuged at 4 °C. All serum samples were stored at -80 °C until use. The serum levels of diamine oxidase (DAO) were measured using an enzyme-linked immunosorbent assay (ELISA; Novus Biologicals™ Rat DAO ELISA Kit [Thermo Fisher Scientific Inc., Waltham, MA, USA]) according to the manufacturer's protocol.

Histological analysis

For the histological analysis of the liver tissue, we evaluated the degree of lipid accumulation (steatosis score), the number of positive macrophages or T lymphocytes in 10 randomly selected fields (lobular inflammation score) using the NAFLD activity score [8].

RNA extraction, reverse transcription and real-time polymerase chain reaction (PCR)

The intestines were frozen at $-80\text{ }^{\circ}\text{C}$ in RNA later TM Soln (Thermo Fisher Scientific Inc.) and batch processed by thawing, transferred to a TRIzol reagent (Thermo Fisher Scientific Inc.), homogenized in a POLYTRON homogenizer (KINEMATICA AG Inc., Malters, Werkstrasse, Switzerland), and the mRNA was extracted using the PureLinkTM RNA MIini Kit (Thermo Fisher Scientific Inc.). Chloroform was added, mixed vigorously for at least 15 s, and then was allowed to stand at room temperature for 3 min. Centrifugation was performed at $4\text{ }^{\circ}\text{C}$, $12,000\times\text{g}$ for 15 min to separate the water layer (upper layer) and organic layer (lower layer). We then transferred 400 μL of the upper layer to a 1.5-mL micro tube, added an equal volume of 70% ethanol, and stirred for 15 s, after which we transferred 700 μL of the sample to a Spin Cartridge, centrifuged at $20\text{ }^{\circ}\text{C}$, $12,000\times\text{g}$ for 15 s, and the residual proteins, phenol, and other contaminants on the column while washing. RNA was purified by adding RNase-free water to the spin cartridge and the RNA content in the extracted sample was determined using an RNA Nano Drop ultra-trace spectrophotometer (Thermo Fisher Scientific Inc.). The RNA concentration was adjusted to 200 ng/ μL with RNase-free dH₂O, and complementary DNA was synthesized using Prime Script RT TM Master Mix (Takara Bio Inc., Kusatsu, Japan).

Quantitative PCR was performed using TB Green Premix EX Taq II (Takara Bio, Inc.). The expression of target genes

was analyzed using the QuantStudio 3 system (Thermo Fisher Scientific Inc.). Forty cycles of PCR were performed and the control group was set at a relative ratio of 1. The primers used in this study were purchased from Takara Bio Inc. All primers used are listed in Table 1a.

Western blot

The liver tissue was homogenized in a solution of T-per™ (Thermo Fisher Scientific, MA, USA) plus cOmplete mini tablets™ (Roche Diagnostics Inc., Basel, Switzerland). The solution was then centrifuged ($10,000\times\text{g}$, 5 min, $4\text{ }^{\circ}\text{C}$), and then the supernatant was mixed with Sample Buffer, and finally boiled at $100\text{ }^{\circ}\text{C}$ for 5 min. The details of the process was conducted in a similar manner to previous studies [9]. All antibodies used in this study are purchased from Abcam Inc. All antibodies used are listed in Table 1b.

Statistical analyses

The data are presented as the mean \pm standard error. Statistical analyses were performed using a two-factor factorial analysis of variance, followed by Tukey’s multiple-comparison test. All results were considered to be statistically significant when the *p*-value was <0.05 .

All statistical analyses were performed using EZR (Saitama Medical Center, Jichi Medical University, Saitama, Japan), a graphical user interface for R (R Foundation for Statistical Computing, Vienna, Austria). More precisely, it is

Table 1 Primer and antibody

Target	Forward	Reverse		
<i>a. Primer for PCR</i>				
PPIA (KEEPING)	5'-GGCAAATGCTGGACCAAACAC-3'	5'-AAACGCTCCATGGCTTCCAC-3'		
Bak1	5'-CGCTACGACACGGAGTTCCA-3'	5'-CCAGCTGATGCCGCTCTTAAATA-3'		
Bcl2	5'-CTGAACCGGCATCTGCACA-3'	5'-CTGAGCAGCGTCTTCAGAGACA-3'		
Bcl2l1	5'-CTTCAGCCACCATTGCTACCAG-3'	5'-CCGTCTAGGCCCAACCCTATAA-3'		
Atg14	5'-CACACAGGCTGCTTTACATGGTC-3'	5'-CGAACCCTGCCTAATGCTGA-3'		
Bax	5'-TGGCGATGAACTGGACAACAA-3'	5'-GGGAGTCTGTATCCACATCAGCA-3'		
Fas	5'-AGGCTCCAGGAATGACTGCTC-3'	5'-CGAGATGCAATCACTAAGCCAAG-3'		
Tnf	5'-CTCCGGGCTCAGAATTTCCA-3'	5'-ATCGACATTCCGGGATCCAG-3'		
Casp3	5'-GCAGCAGCCTCAAATTGTTGAC-3'	5'-TGCTCCGGCTCAAACCATC-3'		
Casp9	5'-CCCAGTGACATCCTTGTGTCCTA-3'	5'-GACACCATCCAAGGTCTCGATGTA-3'		
Tgfb1	5'-CATTGCTGTCCCGTGCAGA-3'	5'-GGTAACGCCAGGAATTGTTGCTA-3'		
Antibody	Host	Company	Catalog	Notes
<i>b. Antibody for western blot</i>				
Anti-Rubicon/Baron	Rabbit	Abcam	ab156052	WB (1:1000)
Anti-SQSTM1/p62	Rabbit	Abcam	ab109012	WB (1:1000)
Anti-LC3B antibody-N-terminal	Rabbit	Abcam	Ab229327	WB (1:1000)
β -actin	Rabbit	Cell signaling	4970	WB (1:1000)

a modified version of the R commander, which is designed to add statistical functions that are frequently used in biostatistics [10].

Ethical approval

This experiment was conducted in accordance with the ARRIVE guidelines and is described in the text according to the checklist. All experimental procedures were approved by the Laboratory Animal Committees of Kagoshima University Graduate School of Medical and Dental Sciences and performed in accordance with the “Guidelines for the Care and Use of Laboratory Animals” (approval number: MD20014).

Results

Body weight and liver weight

The body weight and liver weight are shown in Table 2. The body weights before surgery and at sacrifice did not differ between the two groups. The liver weight and liver-body weight ratio also did not differ between the two groups, but the control group, which showed hepatic steatosis, began to change more than at 1 week than the HGF group.

Histological findings of liver tissue and the analysis based on nonalcoholic fatty liver disease activity score

The histological findings of hematoxylin–eosin staining are shown in Fig. 1. Hepatic steatosis and inflammatory cell infiltration were observed in both groups. However, the HGF group showed significantly less hepatic steatosis (Control group vs. HGF group: 1.4 ± 0.7 vs. 0.2 ± 0.4 , $p < 0.01$) and inflammatory cell filtration (Control group vs. HGF group: 2.4 ± 0.7 vs. 0.8 ± 0.7 , $p < 0.01$) than the control group.

Biochemical assessments

The biochemical assessments are shown in Fig. 2. Inflammatory cytokines tended to be higher in the HGF group than in the control group, although there was no significant difference between the two groups [IL-6: control group vs. HGF

group; 41.7 ± 24.2 vs. 86.3 ± 64.7 , $p = 0.08$], [TNF α : control group vs. HGF group; 6.0 ± 2.9 vs. 8.4 ± 6.8 , $p = 0.474$].

Gene expressions using real-time polymerase chain reaction

The gene expressions using real-time polymerase chain reaction in liver tissue are shown in Fig. 3. Regarding the intrinsic pathway, the HGF group showed a decreasing tendency in the BAX/Bcl2 compared to the control group, but the difference was not significant (Control group vs. HGF group: 5.1 ± 9.8 vs. 0.7 ± 0.4 , $p = 0.24$). The HGF group showed a decreasing tendency in caspase 9 compared to the control group, but the difference was not significant (Control group vs. HGF group: 5.3 ± 8.1 vs. 1.1 ± 0.7 , $p = 0.13$). Regarding the extrinsic pathway, the HGF group showed an increasing tendency in TNF- α compared to the control group, but the difference was not significant (control group vs. HGF group: 2.1 ± 1.4 vs. 6.5 ± 7.0 , $p = 0.13$). The fas ligand expression did not differ between the two groups (Control group vs. HGF group: 1.1 ± 0.5 vs. 1.1 ± 0.4 , $p = 0.65$). The HGF group showed a significant decrease in transforming growth factor $\beta 1$ compared to the control group (control group vs. HGF group: 1.7 ± 0.4 vs. 0.7 ± 0.5 , $p < 0.01$). The caspase 3 expression did not differ between the two groups (control group vs. HGF group: 1.4 ± 2.0 vs. 1.0 ± 1.1 , $p = 0.65$).

Protein expression levels of autophagy using Western blotting

The protein expression levels of autophagy using Western blotting are shown in Fig. 4. The rubicon protein expressions in the HGF group were significantly higher than those in the control group (Control group vs. HGF group: 1.0 ± 0.3 vs. 1.4 ± 0.5 , $p = 0.03$). The p62 protein expressions in the HGF group were significantly higher than those in the control group (Control group vs. HGF group: 0.6 ± 0.1 vs. 2.8 ± 1.3 , $p < 0.01$). The LC3-I protein expressions were not significantly different between the two groups (Control group vs. HGF group: 2.1 ± 0.7 vs. 2.4 ± 1.4 , $p < 0.58$). The LC3-II protein expressions in the HGF group tended to increase more than those in the control group (Control group vs. HGF group: 1.0 ± 0.6 vs. 0.6 ± 0.1 , $p = 0.06$).

Table 2 Changes in body weight and liver weight at sacrifice

	TPN+SBS	TPN+SBS+HGF	<i>p</i> -value
Body weight before surgery, (g)	284.2 ± 31.2	281.6 ± 28.6	0.861
Body weight at sacrifice, (g)	287.2 ± 20.5	285.9 ± 14.8	0.884
Liver weight at sacrifice, (g)	12.8 ± 3.5	11.9 ± 2.7	0.563
Liver/body weight at sacrifice, (%)	4.5 ± 1.2	4.1 ± 0.9	0.534

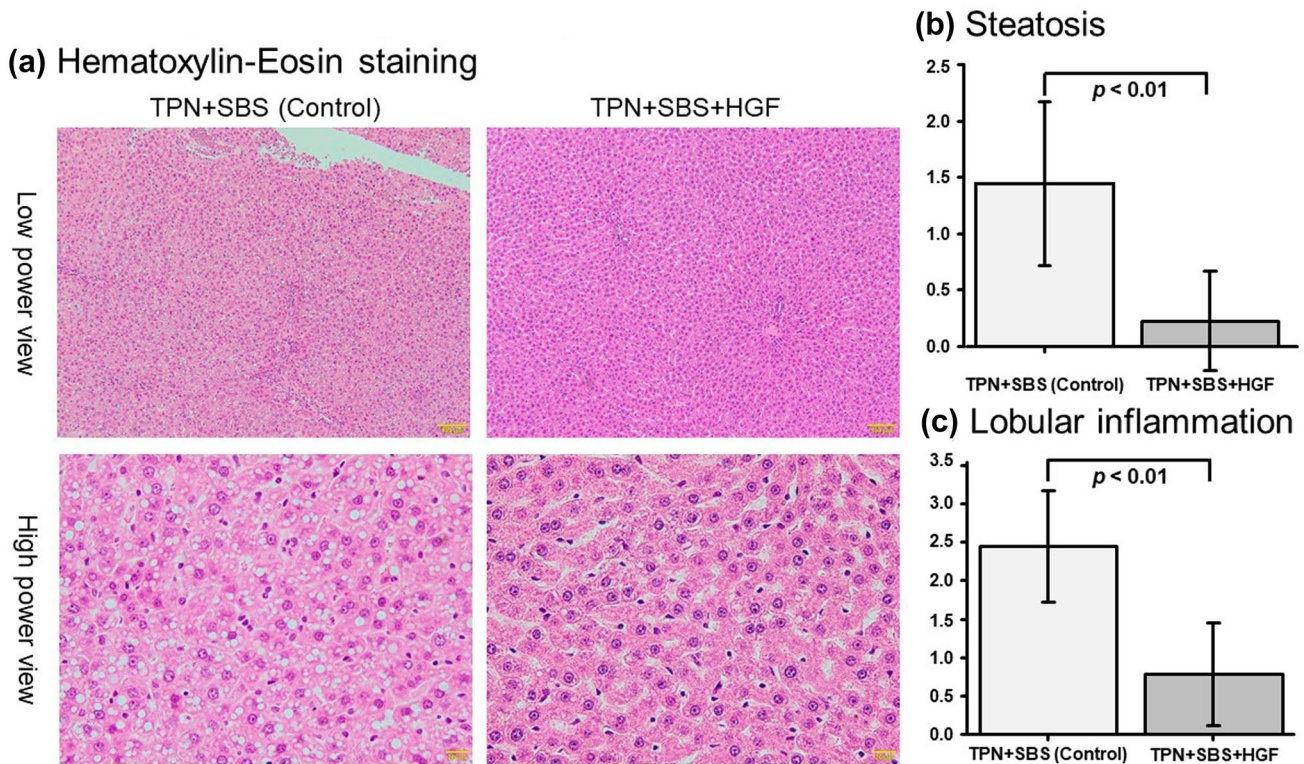


Fig. 1 Histological findings of liver specimens. **a** Hematoxylin–Eosin staining, left column: TPN+SBS (Control), right column: TPN+SBS+HGF, Top Row: Low power view (×40), Bottom Row: High power view (×200), **b** Steatosis, **c** Lobular inflammation

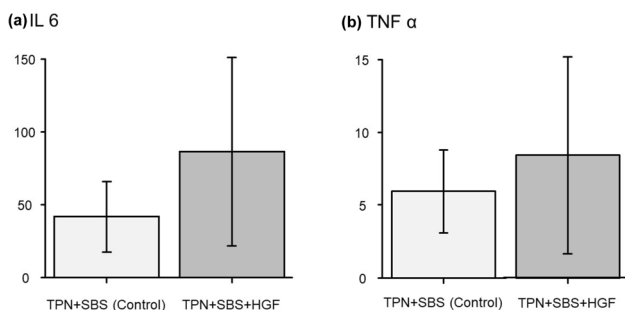


Fig. 2 Biochemical assessment. **a** IL 6, **b** TNF α

Discussion

The major findings of this study are as follows: (1) In an SBS rat model, hepatic steatosis and lobular inflammation in the liver tissue were observed at 1 week, and both were histologically suppressed in the HGF group. (2) The serum inflammatory cytokines were not suppressed in the HGF group at 1 week, and TNFα remained high tendency in the liver tissue. (3) tgfb in the HGF group was suppressed compared to the control group. (4) The HGF group showed a decreasing tendency in caspase 9 compared to

the control group. (5) Protein expressions of Rubicon and P62 in liver tissue in the HGF group were found to have increased compared to those in the control group.

We prepared a 1-week TPN plus SBS fasting model focusing on early postoperative liver injury. In this model, the inflammatory responses in rats, including the liver tissue, were higher in the HGF group. Katz et al. reported that HGF suppressed TNF-α and IL-6 in a volume-dependent manner in a 2-week study in a 70% SBS plus TPN rat model based on immunohistochemical staining [11]. Differences in inflammatory response results may be due to differences in the number of weeks in the model or the length of the bowel resection. The HGF group with high inflammation had the potential to promote apoptosis via an extrinsic caspase pathway induced by TNF-α, but there was no increase in caspase3. This may be the result of the anti-apoptotic effect of HGF on the endogenous pathway [4, 12]. The strong anti-apoptotic effect of HGF may be limited in the early stages of short bowel syndrome due to high inflammation. TGF-β causes increased vascular resistance in injured liver tissue and portal vein pressure [13]. In chronic liver injury, TGF-β is also an important factor in the activation of hepatic stellate cells, resulting in a reduced resistance to oxidative stress and liver fibrosis. HGF has an antagonistic effect on TGF-β [14]; therefore,

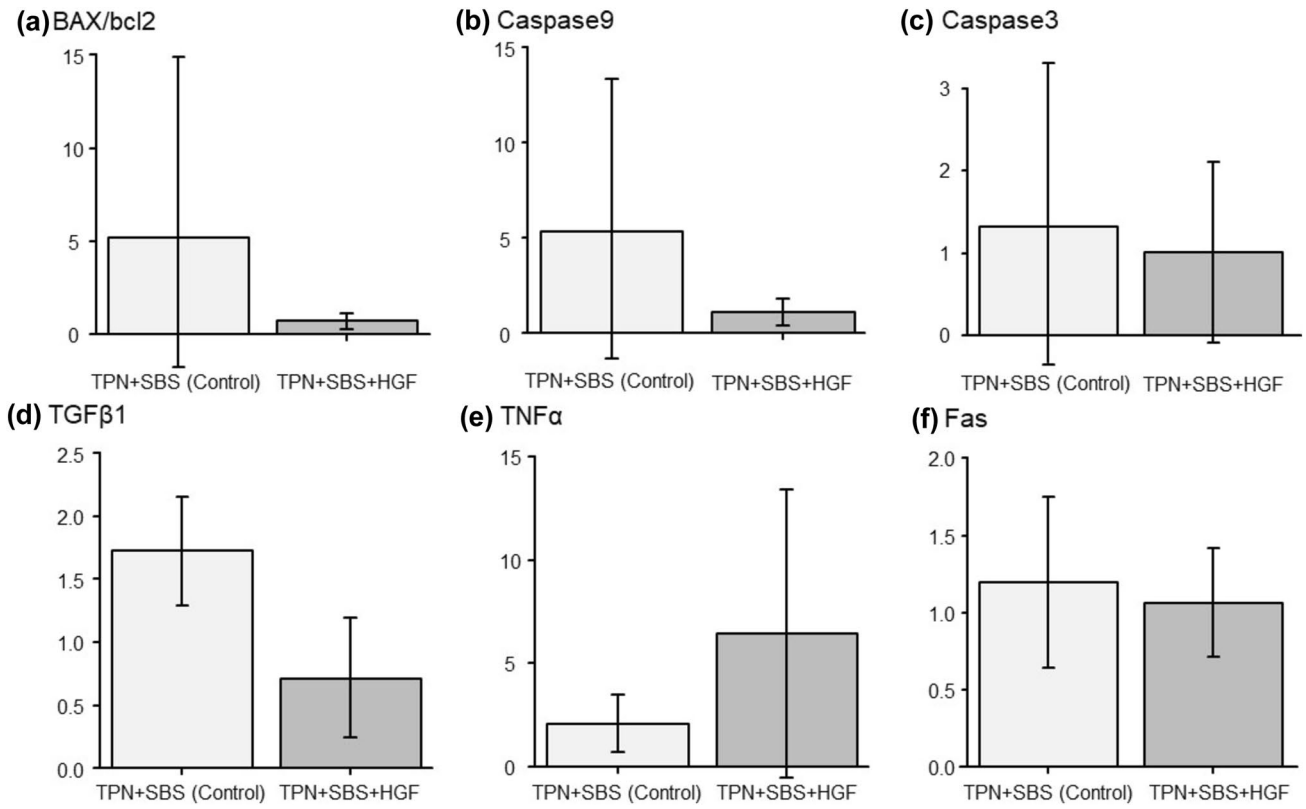


Fig. 3 Gene expressions using real-time polymerase chain reaction. **a** BAX/bcl2, **b** Caspase9, **c** Caspase3, **d** TGFβ, **e** TNFα, **f** Fas

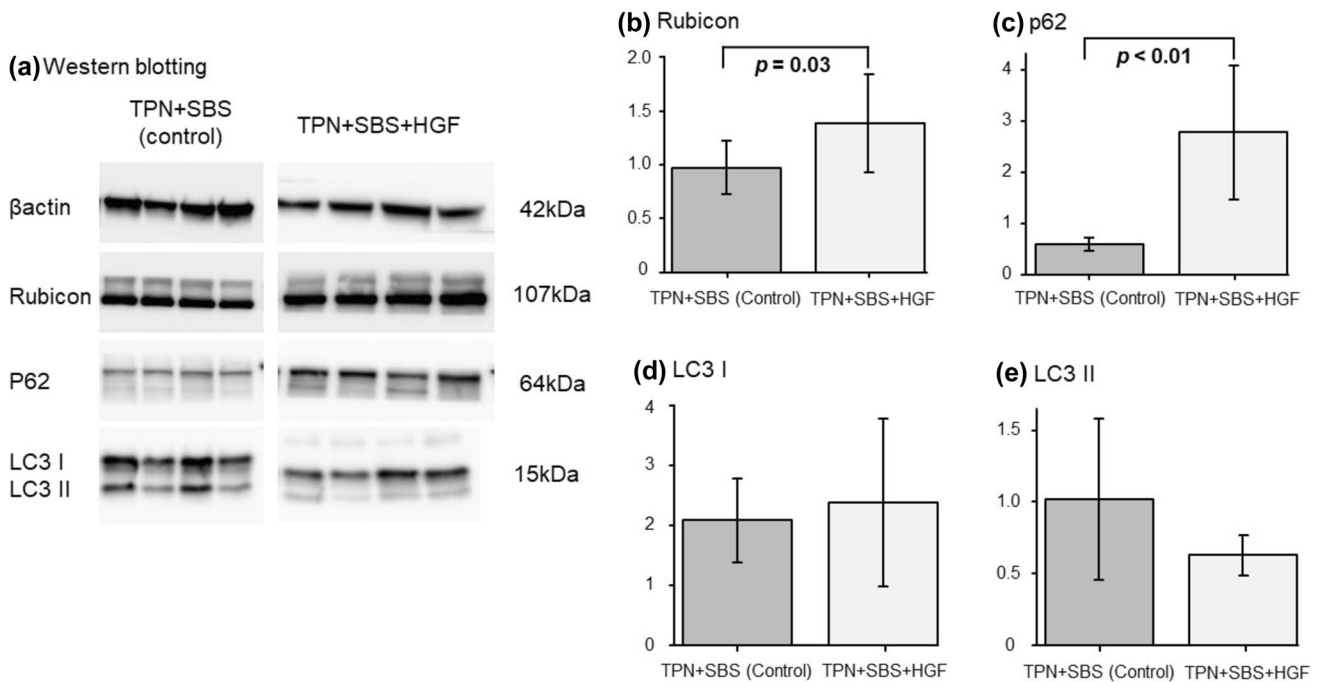


Fig. 4 Protein expression levels of autophagy using Western blotting. **a** Western blotting, left column: TPN+SBS (Control), right column: TPN+SBS+HGF; **b** Rubicon, **c** p62, **d** LC3 I, **e** LC3 II

the effect of HGF through TGF- β suppression may be effective in chronic or rapidly deteriorating IFALD.

Accumulated hepatic steatosis is induced by autophagy and apoptosis, and the chronic process leads to inflammation and fibrosis. It has been reported that in NAFLD, Rubicon suppresses autophagy and it enhances apoptosis [15]. In the present study, despite the fact that HGF treatment increased Rubicon protein expression and inhibited apoptosis, no fat deposition was observed. In this study, it is unclear the impact of autophagy in the control group, it is speculated that autophagy may not be occurring in the HGF group. The mechanisms underlying the action of HGF on Rubicon and autophagy remain unclear in the present study. However, since HGF maintains the mTOR activity via PI3K-Akt signaling [16, 17], HGF may suppress the mTOR-dependent macroautophagic process (main autophagy process) and protect hepatocytes. In other words, increased the protein of Rubicon and P62 may only be seen as a result of decreased autophagy.

If lipolysis does not occur, then HGF may inhibit fat accumulation, which is a subject for future research. The main mechanisms of fat accumulation in the liver are abnormal glucose levels and an abnormal lipid metabolism, increased insulin resistance, and increased triglyceride levels. Therefore, it is likely that HGF acts on one of these pathways. HGF has been reported to promote intestinal adaptation in an SBS model. Intestinal adaptation protects liver metabolism and inflammation via the intestine-liver axis [18–22]. In this study, HGF may also have reduced hepatic steatosis by promoting intestinal adaptation, relying solely on intestine-liver axis signaling. Fafalios et al. reported that HGF restored insulin responsiveness in a mouse model of insulin refractoriness [23]. HGF regulates the metabolism by stimulating the hepatic glucose uptake and inhibiting the hepatic glucose production. The results of the HGF group may indicate that metabolism in the liver tissue is working normally. The process of HGF acting on the pathways of hepatic metabolism must be investigated.

Limitations

Although there was some scattering in the data, we refrained from using more animals than we had previously prepared for this experiment based on animal ethics. Due to the limited number of animals, statistical interpretation was limited.

Conclusions

HGF does not cause autophagic lipolysis. The inhibitory effect of HGF on hepatic steatosis remains unclear, and further studies focusing on the mechanisms of fat accumulation are needed.

Acknowledgements This work was supported by the Laboratory Animal Science Research Support Center Institute for Research Promotion, Kagoshima University. We thank Mr. Brian Quinn for his comments and assistance with this manuscript. We thank Tomomi Kamibayashi, a technician at our institution, for her help with the rat's management, histopathological measurement, biological measurement, western blot, and RT-PCR analyses. We thank Orié Iwaya, a technician at the Department of Pathology, Graduate School of Medical and Dental Science, for her help with histopathological staining. This study was supported by Grants-in-Aid for Scientific Research from the Japan Society for the Promotion of Science (JSPS: 23K08031, 22K07848, 22K07894, 22K08719, 22K08736, 22K08757, 21K07867, 21K08623) and a Grant from the Kawano Masanori Memorial Foundation for Promotion of Pediatrics.

Author contribution KS, KY, and MM designed the study. KS, KY, SO, and TK performed experiments. YI, MO, and LT supported histopathological assessment. MM, TH, and KS analyzed the data and created the Figure. MM, KK, AI, and TK provided conceptual advice. KS wrote the manuscript in consultation with SI.

Data availability The datasets generated and/or analyzed during the current study are available from the corresponding author upon reasonable request.

Declarations

Conflict of interest The authors declare no conflicts of interest in association with the present study.

References

1. Thatch KA, Schwartz MZ, Yoo EY, Mendelson KG, Duke DS (2008) Modulation of the inflammatory response and apoptosis using epidermal growth factor and hepatocyte growth factor in a liver injury model: a potential approach to the management and treatment of cholestatic liver disease. *J Pediatr Surg* 43(12):2169–2173
2. Sugimoto T, Yamashita S, Ishigami M, Sakai N, Hirano K, Tahara M, Matsumoto K, Nakamura T, Matsuzawa Y (2002) Decreased microsomal triglyceride transfer protein activity contributes to initiation of alcoholic liver steatosis in rats. *J Hepatol* 36(2):157–162
3. Kosone T, Takagi H, Horiguchi N, Ariyama Y, Otsuka T, Soharu N, Kakizaki S, Sato K, Mori M (2007) HGF ameliorates a high-fat diet-induced fatty liver. *Am J Physiol Gastrointest Liver Physiol* 293(1):G204–210
4. Matsukubo M, Yano K, Kaji T, Sugita K, Onishi S, Harumatsu T, Nagano A, Matsui M, Murakami M, Yamada K, Yamada W, Muto M, Kumagai K, Ido A, Ieiri S (2021) The administration of hepatocyte growth factor prevents total parenteral nutrition-induced hepatocellular injury in a rat model. *Pediatr Surg Int* 37(3):353–361
5. Yano K, Kaji T, Onishi S, Machigashira S, Nagai T, Harumatsu T, Yamada K, Yamada W, Muto M, Nakame K, Mukai M, Ieiri S (2019) Novel effect of glucagon-like peptide-2 for hepatocellular injury in a parenterally fed rat model of short bowel syndrome. *Pediatr Surg Int* 35(12):1345–1351
6. Yano K, Sugita K, Muto M, Matsukubo M, Onishi S, Kedoin C, Matsui M, Murakami M, Harumatsu T, Yamada K, Yamada W, Kumagai K, Ido A, Kaji T, Ieiri S (2022) The preventive effect of recombinant human hepatocyte growth factor for hepatic steatosis in a rat model of short bowel syndrome. *J Pediatr Surg* 57(7):1286–1292

7. Sugita K, Kaji T, Yano K, Matsukubo M, Nagano A, Matsui M, Murakami M, Harumatsu T, Onishi S, Yamada K, Yamada W, Muto M, Kumagai K, Ido A, Ieiri S (2021) The protective effects of hepatocyte growth factor on the intestinal mucosal atrophy induced by total parenteral nutrition in a rat model. *Pediatr Surg Int* 37(12):1743–1753
8. Nabeshima A, Yamada S, Guo X, Tanimoto A, Wang KY, Shimajiri S, Kimura S, Tasaki T, Noguchi H, Kitada S, Watanabe T, Fujii J, Kohno K, Sasaguri Y (2013) Peroxiredoxin 4 protects against nonalcoholic steatohepatitis and type 2 diabetes in a non-genetic mouse model. *Antioxid Redox Signal* 19(17):1983–1998
9. Nishikoba N, Kumagai K, Kanmura S, Nakamura Y, Ono M, Eguchi H, Kamibayashiyama T, Oda K, Mawatari S, Tanoue S, Hashimoto S, Tsubouchi H, Ido A (2020) HGF-MET signaling shifts m1 macrophages toward an M2-like phenotype through PI3K-mediated induction of arginase-1 expression. *Front Immunol* 11:2135
10. Kanda Y (2013) Investigation of the freely available easy-to-use software “EZ” for medical statistics. *Bone Marrow Transplant* 48(3):452–458
11. Katz MS, Thatch KA, Schwartz MZ (2010) Dose variation of hepatocyte growth factor and its effects on an animal model of TPN-induced liver injury. *J Surg Res* 163(2):294–298
12. Gao M, Fan S, Goldberg ID, Latterra J, Kitsis RN, Rosen EM (2001) Hepatocyte growth factor/scatter factor blocks the mitochondrial pathway of apoptosis signaling in breast cancer cells. *J Biol Chem* 276(50):47257–47265
13. Puche JE, Saiman Y, Friedman SL (2013) Hepatic stellate cells and liver fibrosis. *Compr Physiol* 3(4):1473–1492
14. Narmada BC, Chia SM, Tucker-Kellogg L, Yu H (2013) HGF regulates the activation of TGF-beta1 in rat hepatocytes and hepatic stellate cells. *J Cell Physiol* 228(2):393–401
15. Tanaka S, Hikita H, Tatsumi T, Sakamori R, Nozaki Y, Sakane S, Shiode Y, Nakabori T, Saito Y, Hiramatsu N, Tabata K, Kawabata T, Hamasaki M, Eguchi H, Nagano H, Yoshimori T, Takehara T (2016) Rubicon inhibits autophagy and accelerates hepatocyte apoptosis and lipid accumulation in nonalcoholic fatty liver disease in mice. *Hepatology* 64(6):1994–2014
16. Moumen A, Patane S, Porras A, Dono R, Maina F (2007) Met acts on Mdm2 via mTOR to signal cell survival during development. *Development* 134(7):1443–1451
17. Gallo S, Gatti S, Sala V, Albano R, Costelli P, Casanova E, Comoglio PM, Crepaldi T (2014) Agonist antibodies activating the Met receptor protect cardiomyoblasts from cobalt chloride-induced apoptosis and autophagy. *Cell Death Dis* 5(4):e1185
18. Bagias G, Misiakos EP, Charalampopoulos A, Zavras N, Sakellariou S, Schizas D, Sukhotnik I, Giamarellos E, Pikoulis E (2023) The effect of hepatocyte growth factor on intestinal adaptation in an experimental model of short bowel syndrome. *Pediatr Surg Int* 39(1):80
19. Schwartz MZ, Kato Y, Yu D, Lukish JR (2000) Growth-factor enhancement of compromised gut function following massive small-bowel resection. *Pediatr Surg Int* 16(3):174–175
20. Kato Y, Yu D, Schwartz MZ (1998) Enhancement of intestinal adaptation by hepatocyte growth factor. *J Pediatr Surg* 33(2):235–239
21. Kato Y, Yu D, Schwartz MZ (1998) Hepatocyte growth factor up-regulates SGLT1 and GLUT5 gene expression after massive small bowel resection. *J Pediatr Surg* 33(1):13–15
22. Kato Y, Yu D, Lukish JR, Schwartz MZ (1997) Hepatocyte growth factor enhances intestinal mucosal cell function and mass in vivo. *J Pediatr Surg* 32(7):991–994
23. Fafalios A, Ma J, Tan X, Stoops J, Luo J, Defrances MC, Zarnegar R (2011) A hepatocyte growth factor receptor (Met)-insulin receptor hybrid governs hepatic glucose metabolism. *Nat Med* 17(12):1577–1584

Publisher's Note Springer Nature remains neutral with regard to jurisdictional claims in published maps and institutional affiliations.

Springer Nature or its licensor (e.g. a society or other partner) holds exclusive rights to this article under a publishing agreement with the author(s) or other rightsholder(s); author self-archiving of the accepted manuscript version of this article is solely governed by the terms of such publishing agreement and applicable law.